Study of CORC Conductors With Respect to Individual Tape Properties

A. Torre, J. Pavan, B. Lacroix, C. Nguyen Thanh Dao, V. Corato, and D.C. van der Laan, *Senior Member, IEEE*

***Abstract*—CEA has been studying the advantages of a conductor based on an assembly of CORC cables in the high field zone of a hybrid Central Solenoid (CS) magnet for EU-DEMO. To this end, the detailed study of geometrical and electrical parameters of a CORC structure are studied in order to evaluate the cable's electrical performance as well as to determine a number of important parameters (crossing points, contact surface etc…) as function of the cable structure. The paper first presents these geometrical and performance analyses. It will then try to introduce smeared models in order to reduce the cable's performance to 1D tape scaling law using effective parameters. That reduction is of importance for use in thermohydraulic models. Finally, the paper will present the case study of a particular CORC conductor that is being procured and is foreseen to be tested in SULTAN in 2025. The paper will try to give some predictive estimate of the cable performance and identify some of the unknowns related to current redistribution and joint resistance.**

***Index Terms*—Superconductors, HTS, CORC.**

I. Introduction

In THE framework of the Eurofusion WPMAG activities, CEA has started working on the design of a hybrid CS magnet [1], with inner turns based on conductors using CORC sub-cables.

II. CORC Structure

A. Layers Geometrical Description

In order to describe a CORC structure, we can define a reduced set of parameters. Each layer, of index i, is fully described by 2 parameters related to the tape : *[Th_{Li}, W_{Li}]*, respectively the thickness and width of the tapes in this layer, and 3 parameters related to the layer: *[R_{Li}, Lp_{Li}, Nt_{Li}]*, respectively the inner radius of this layer, the twist pitch of the tapes and the number of tapes in this layer. From these, we can define easily the twist angle: $\alpha_{Li} = \text{atan}(2\pi R_{Li}/Lp_{Li})$, as well as the width of the tape in a transverse cross-section $W_{Li}' = W_{Li}/\cos(\alpha_{Li})$. The gap between tapes is also given by:

$$\boldsymbol{e_{Li}} = 2\pi\ R_{Li} \cos\left(\text{atan}\left(\frac{2\pi R_{Li}}{Lp_{Li}}\right)\right)/Nt_{Li} - W_{Li} \quad (1)$$

Now the inter-tape gap is an important parameter for this type of cable mechanical stability, and it might even be more important to specify the gap e_{Li} and deduce the twist pitch inversing (1):

$$\boldsymbol{Lp_{Li}} = \pm\frac{2\pi R_{Li}(e_{Li}+W_{Li})Nt_{Li}}{\sqrt{(2\pi R_{Li})^2-(e_{Li}+W_{Li})^2 Nt_{Li}^2}} \quad (2)$$

The +/− sign in (2) defines the layer cabling direction (clockwise or anti-clockwise). It is thus possible to define a matrix describing the CORC structure, as illustrated in Fig. 1, where each line is a layer, and columns contain the parameters [*Th_{Li}, W_{Li}, R_{Li}, e_{Li}, Nt_{Li}*].

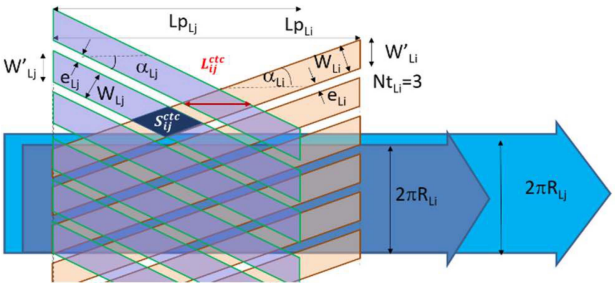

Fig. 1. Illustration of crossing layers (i and j) parameters.

B. Geometrical Features

Some additional geometrical features can be of interest, especially if one foresees to model the contact between tapes of adjacent layers (for electrical, hydraulic or mechanical simulation). If one was to take successive layers (i,j), the contact length and surface area at the crossing of two tapes is given by (3) and (4):

$$\boldsymbol{L_{ij}^{ctc}} = \frac{(WLj' + WLi')}{2\pi}\left(\frac{LpLj.LpLi}{LpLi.RLj + LpLj.RLi}\right) \quad (3)$$

Received 16 July 2025; revised 8 October 2025; accepted 17 October 2025. Date of publication 22 October 2025; date of current version 17 November 2025. This work was supported in part by European Union via the Euratom Research and Training Programme through EUROfusion Consortium under Grant Agreement 101052200 — EUROfusion and in part by the French National Research Agency through France 2030 Program, under Reference 'ANR-24-EXSF-0003'. *(Corresponding Authors: A. Torre.)*

A. Torre, J. Pavan, B. Lacroix, and C. Nguyen Thanh Dao are with CEA, IRFM, Centre de Cadarache, 13108 Saint-Paul-lez-Durance, France (e-mail: Alexandre.TORRE@cea.fr; Jonathan.PAVAN@cea.fr; Benoit.LACROIX@cea.fr; Clement.NGUYENTHANHDAO@cea.fr).

V. Corato is with the Energy and Sustainable Economic Development, ENEA (Italian National Agency for New Technologies), 00196 Roma, Italy (e-mail: valentina.corato@enea.it).

D.C. van der Laan is with Advanced Conductor Technologies LLC, Boulder, CO 80301 USA (e-mail: danko@advancedconductor.com).

Color versions of one or more figures in this article are available at https://doi.org/10.1109/TASC.2025.3624351.

Digital Object Identifier 10.1109/TASC.2025.3624351

$$\boldsymbol{S_{ij}^{ctc}} = \frac{W_{Lj} W_{Li}}{\sin\left(\frac{\pi}{2} - (\alpha_{Li} + \alpha_{Lj})\right)} \tag{4}$$

In preparation for a potential electrical model, it can be important to know the longitudinal position of the contact points between tapes in adjacent layers. For this we can define the parametric equation of tape k_i (centerline) in layer i, where z is the longitudinal coordinate, and θ_{0i} is the phase angle of this particular layer :

$$\theta_{\boldsymbol{ki}} = \theta_{0i} + \left(\frac{2\pi}{NtLi}\right) k_i \mp \frac{2\pi z}{LpLi} \; (k_i = 0 \; to \; Nt_{Li} - 1) \tag{5}$$

The +/- sign deals with layers with clockwise or anti-clockwise twisting. For tapes (k_i,k_j), (6) gives the tapes centerline crossing point z-coordinates, where γ is an integer and *ki* and *kj* range from 0 to (*NtL*-1):

$$\boldsymbol{z_{kj}^{ki}} = \frac{Lp_{Lj}.Lp_{Li}}{(Lp_{Lj} + Lp_{Li})} \times \left(\left(\theta_0^{Layj} - \theta_0^{Layi}\right)/2\pi + (k_j/Nt_{Lj} - k_i/Nt_{Li}) + \gamma\right) \tag{6}$$

III. Scaling Law and Limiting Cases

A. Scaling Law and Lift Factors

In order to start looking at a cable expected performance, a critical current scaling law describing the full $J_C(B,T,\varphi)$ critical surface, including the angular dependence, was needed. After a review of existing scaling laws, we chose the formula proposed by CERN in 2014 [1], with the following general expression:

$$\boldsymbol{J_C}\ (\boldsymbol{B},\boldsymbol{T},\boldsymbol{\theta}) = J_{C,c}\ (B,T) + \frac{J_{C,ab}\,(B,T) - J_{C,c}\,(B,T)}{1 + \left(\frac{\theta - \pi/2}{g(B,T)}\right)^{\nu}} \frac{A}{m^2} \tag{7}$$

The parameters, as defined in [2], were for a Fujikura tape of 10 mm width. The cable ordered to Advanced Conductor Technology (ACT) will use Shanghai Superconducting Technology (SST) tapes, and thus the scaling law needed to be adapted. Based on experimental values and lift factors (ratio of operating I_C to 77 K I_C at self-field = SF) provided by SST, we fitted a reduced set of points (see Fig. 2) and got the following scaling parameters (see Table I) with an overall good fit agreement (below 10% error). We should mention that we had a range of expected 77 K properties (and thus lift factors) and we considered only the most conservative value (156 A@77 K, SF).

B. Single Tape Twist, Critical Current and Effective Angle

For a single tape twisted on a cylindrical core (defined by [Th_{Li}, W_{Li}, R_{Li}, e_{Li}, Nt_{Li}]), the angular width seen by the tape in a cross-section is easily found: $\Delta\theta_{Li} = W'_{Li}/R_{Li}$. If one considers the tape equipotential in the cross-section (free current distribution), the local tape critical current at longitudinal position z can be found by the (8), permitting to define a local

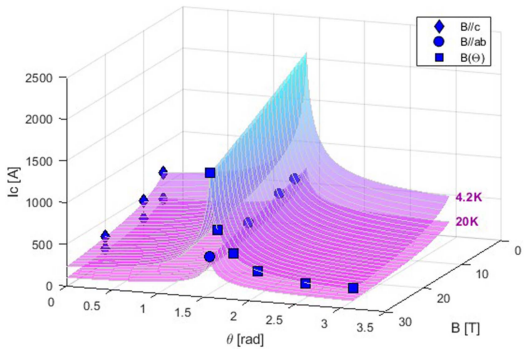

Fig. 2. Illustration of the experimental points and fit at 4.2 K and 20 K.

TABLE I
SST Tape Considered: Scaling Law Parameters

General parameters			ab-axis parameters			θ sensitivity		
T_{C0}	[K]	93	$B_{i0,ab}$	[T]	250	ν	[-]	0.857
n	[-]	1	$\alpha_{\alpha\beta}$	[MA.T/mm^2]	84	g_0	[-]	-0.005
c-axis parameters			p_{ab}	[-]	1.02	g_1	[-]	0.094
$B_{i0,c}$	[T]	140	q_{ab}	[-]	4.45	g_2	[-]	-0.0008
α_χ	[MA.T/mm^2]	1.41	$\gamma_{\alpha\beta}$	[-]	4.73	g_3	[-]	0.0039
p_c	[-]	0.31	n_1	[-]	1.77	**REBCO properties**		
q_c	[-]	0.87	n_2	[-]	4.1	t	[μm]	1.5
γ_χ	[-]	3.09	a	[-]	0.1	w	[mm]	4

effective angle $\theta_{eff}(z)$:

$$\boldsymbol{I_c^{tape}}\ (\boldsymbol{z}) = \frac{R_{Li}\cos(\alpha_{Li})}{W_{Li}} \times \int_{\theta 0 - \frac{\Delta\theta}{2}}^{\theta 0 + \frac{\Delta\theta}{2}} Ic\,(B,T,\theta)\,d\theta = I_c\ (B,T,\theta_{eff}\,(z)) \tag{8}$$

And then, if one wants to compute the overall tape critical current over a given length *L*, (9) can be applied, which can also be used to define an overall effective angle parameter θ_{eff}:

$$\boldsymbol{I_c^{tape}} = \left(L/\int_0^L \left(\frac{1}{I_C^{tape}\,(z)}\right)^n dz\right)^{\frac{1}{n}} = I_c\ (B,T,\theta_{eff}) \tag{9}$$

The definition of such effective parameters is important for 1D simplification of tape properties, either for thermohydraulic or electrical models.

C. Cable Limiting Cases

Such models can also be defined for the cable provided some current distribution hypotheses are defined. In particular, one can define the Low-Resistivity-Limit (LRL) where each cross-section is equipotential, and we define local and overall equivalent cable I_C as in (10):

$$I_{C\ LRL}^{cable} = \left(L/\int_0^L \left(\frac{1}{I_C^{cable}\,(z)}\right)^n dz\right)^{\frac{1}{n}},$$
$$I_C^{cable}\,(z) = \sum_k I_{C\ k}^{tape}\,(z) \tag{10}$$

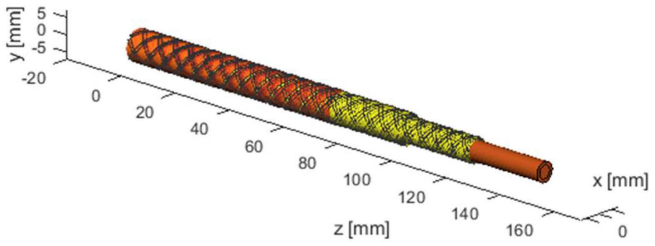

Fig. 3. Illustration of the 20 kA@(18 T,20 K) CORC procured and studied.

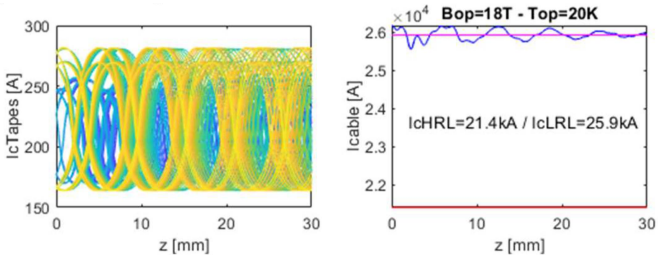

Fig. 4. Individual tapes (left) and cable (right) critical currents.

While the High-Resistivity-Limit (HRL) is defined in (11), where each tape is insulated from its neighbors:

$$I_{C\,HRL}^{cable} = \sum_k I_{C\,k}^{tape},\ I_{C\,k}^{tape} = \left(L / \int_0^L \left(\frac{1}{I_{C\,k}^{tape}(z)} \right)^n dz \right)^{\frac{1}{n}} \tag{11}$$

These two cases are sometimes defined as limiting cases, going from HRL to LRL by decreasing inter-tape resistances. Nevertheless, it should be said that if a current is imposed at boundary conditions (joints for example) the resulting cable critical current can be lower than HRL limit (for example, the cable I_C can be close to the single tape I_C if all current is injected in one specific tape and the inter-tape resistance is high).

IV. Cable and Conductor Performance

A. Cable Considered

In the framework of the WPMAG-Eurofusion activities, the study of a CORC cable as a sub-element of a future LTS-HTS hybrid Central Solenoid (CS) was launched. The CORC procured had technical specifications of 20 kA@(18 T,20 K), and ended being structured with 34 superconducting layers and 120 tapes of 4 mm width, for a total outer diameter of about 10 mm. The central cylinder is a copper tube as represented in Fig. 3.

B. CS Design Point: Critical Current Evaluation

There are several operating conditions that we would like to test, but the initial target was to use this CORC as a sub-element carrying 20 kA in conductor for a hybrid CS generating 18 T background field, at a temperature of 20 K (T_{op} = 5 K and ΔT_{margin} = 15 K). Therefore, we also considered a field gradient B_{grad} of +/- 0.8 T on the width of the cable (which is the self-field for a 100 kA conductor of 50 mm diameter, but also conveniently the self-field of a 20 kA conductor of 10 mm diameter). Applying the methods described above, one can estimate the cable I_C in both limiting cases (LRL/HRL). The baseline computation is made for a 100 mm long cable. Fig. 4 illustrates this computation, which results in $\mathrm{Ic_{LRL/HRL}}$ = [25.9/21.4]kA. The colors in Fig. 4 left plot only represent the index of the tape considered (blue inner layers, yellow outer layers).

This figure highlights a few interesting points:

- Tapes I_C oscillate between 165 A and 270 A taking into account field orientation and field gradient.
- The resulting cable current transport capacity $I_C{}^{cable}(z)$ has a smeared residual oscillation of about 500 A (2%) at the start of the cable, that is decreasing after a few millimeters.
- $I_C{}^{cable}{}_{LRL}$, with perfect current re-distribution, is close to the average longitudinal current transport.
- $I_C{}^{cable}{}_{HRL}$, with no current re-distribution, foresees a 17% I_C reduction compared to LRL.

C. Other Operating Points (OP) of Interest

We will now define a set of important point of interest in the operational window of this cable (see Table II), and for each of these, we will give the $\mathrm{Ic_{HRL/LRL}}$ range, computed as described previously.

While OP1 and OP2 are self-explanatory, OP3 looks at what (maximum) current could be injected in this cable if tested in SULTAN at minimum supercritical helium (SHe) temperature (4.5 K). OP4, inversing the I_C computation, gives the expected T_{CS} if the cable is tested at nominal current in SULTAN. Finally OP5 looks at what should be the injected current in the cable to reproduce the design IxB load (18 T × 20 kA = 360 kN/m) in the lower field of SULTAN (10.7 T × 33.64 kA = 360 kN/m). The expected T_{CS} OP5 is also given. These values will help us define/refine the SULTAN test program.

V. Sensitivity Studies

A. Length Effect

The length of the cable studied can affect the overall I_C because the layer system is only periodic after the product of all layers twist pitches. we also wanted to check if the initial oscillations of the cable $I_C(z)$ would dampen out or repeat themselves. We did the computation for a 5m length cable, and we can confirm that the 500 A $I_C(z)$ oscillation is present all along the cable length. Nevertheless, this does not change the expected I_C (neither LRL nor HRL).

B. Defect Introduction

We know that tapes can have local I_C dropouts that range from few percent to potentially 20–30% (or higher). Furthermore, this type of I_C reduction can also be the result of handling and/or cabling processes. We wanted to know how such local I_C drops would affect expected performances in good (LRL) or bad (HRL) current redistribution hypotheses.

TABLE II
OPERATING POINTS OF INTEREST

Description	Test Conditions or Tcs	$Ic_{[HRL/LRL]}$ or I_{op}
OP1: CS design point	B_{op}=18T/T_{op}=20K	[21.4/25.9]kA
OP2: CS current margin	B_{op}=18T/T_{op}=4.5K	[47.2/61.7]kA
OP3: SULTAN low T	B_{op}=10.7T/T_{op}=4.5K	[61.2/76.3]kA
OP4: SULTAN Tcs	B_{op}=10.7T $Tcs_{HRL/LRL}$=[26.1/27.2]K	20kA
OP5: SULTAN IxB Tcs	B_{op}=10.7T/B_{grad}=+/-1.34T $Tcs_{HRL/LRL}$=[17.7/20.2]K	33.64kA

We thus defined local I_C reduction (in REBCO layer) by introducing the I_C retention coefficient α_{ret} between 0 ($I_C = 0$) and 1 (no defect), and a spatial length of defect repetition $\boldsymbol{L_{def}}$ to vary the spatial frequency of the introduced dropout. The hypothesis here is that defects affect a full cross-section of the tape, and that the spatial period $\boldsymbol{L_{def}}$ is along the curvilinear abscissa of the twisted tape. Finally, in each layer with ***NtLi*** tapes, each tape is affected by the defects distribution, but not in the same cross-section (shifted of LpLi/NtLi to space them out). Fig. 5 shows the computation for $\alpha_{ret} = \boldsymbol{0.7}$and $\boldsymbol{L_{def}} = \boldsymbol{100\ mm}$, with resulting individual tapes I_C map on a 1m long cable (zoom on 50 mm) as well as the full cable current carrying capacity. The dropouts are visible, but the cable resulting $I_{C\ LRL}$ is not affected, while the I_{CHRL} drops by about 6.5% .

One of the remarks one could make considering those results is that the CORC structure already has a quite large I_C distribution because of tape twisting, and dropouts will affect sometimes the low-Ic areas, but also sometimes the high-Ic regions, in which case they won't be affecting much the overall cable I_C. A parametric study of $I_{C\ LRL}/I_{C\ HRL}$ can be made varying α_{ret} and $\boldsymbol{L_{def}}$, with 2D maps illustrated in Fig. 6 representing the impact of defect distribution on cable I_C. The main conclusion is that a good current redistribution is able to cope with many dropouts of significant amplitude while retaining most of its current carrying capacity.

VI. ELECTRICAL NETWORK MODEL : CARMEN

A. Network Architecture and Matrix Generation

Modelling the current redistribution in a CORC$^{@}$ necessitates a resistive network model (see for example [3] or [4]). CARMEN (for *Coupled Algorithm for Resistive Modeling of Electrical Networks*, see [5], [6], [7]) is a code solving Kirchoff's equations in resistive networks that include superconducting parts by the following matrix equation:

$$\begin{bmatrix} M.R \\ Q \end{bmatrix} I = \begin{bmatrix} 0 \\ I_{inj} \end{bmatrix} \tag{12}$$

Where M (tie-set matrix) and Q (cut-set matrix) represent loops and junctions rule respectively, R is the resistance vector, I the currents in the branches and I_{inj} the injected currents. The electrical CORC structure is modelled using 2 inputs: ***NtLi*** vector representing for each layer the number of tapes, and ***ns*** the number of longitudinal sections. Routines were created for generation of (M,Q) for any (*NtLi*, *ns*) structures (see Fig. 7 for an example of CARMEN CORC$^{@}$ network structure).

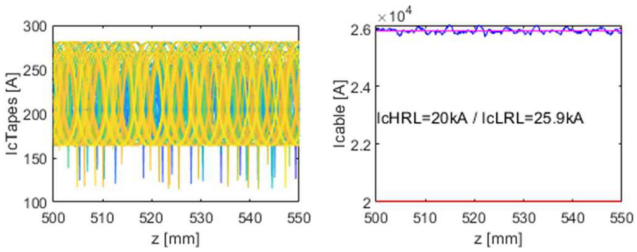

Fig. 5. Individual tapes (left) and cable (right) critical currents.

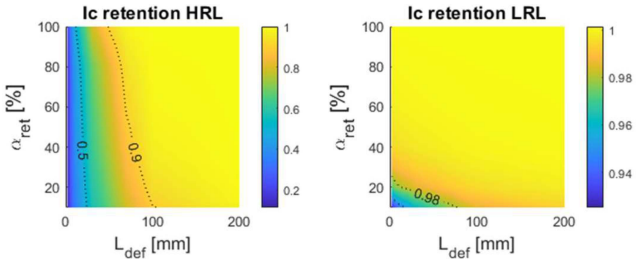

Fig. 6. Cable Ic_{LRL} and Ic_{HRL} retention for combinations of (α_{ret},L_{def}).

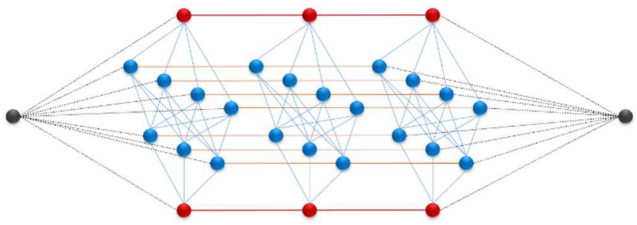

Fig. 7. CORC electrical structure for NtLi = [1; 3; 4; 1] and ns = 2. Red nodes and segments are copper parts, black dashed lines are joint resistances, blue segments are inter-tape connections, and orange segments are superconducting elements.

B. Resistances Estimations and Hypotheses

To fix the branches resistances, we based our models on the following hypotheses:

- Joint resistances R_j are based on an estimated contact surface of tape to the joint of $S_j = 1$ cm^2, soldered (like in CORC terminations), using a contact surface resistance $\rho_j e_j = 1\ \mu\Omega$.cm^2 (in the lower range found in [8]). This gives $R_j = 10^{-7}\ \Omega$ (but can be changed).
- Contact resistances R_{ctc} between tapes in the CORC cable is based on values from [10] and [11]. For pre-tinned tapes, it is about $\rho_c e_c = 1\ \mu\Omega$.cm^2. Using (4) for $S^{ij}{}_{ctc}$ from Section II, we deduce R_{ctc} locally. A search of contacts/connections between tapes is necessary and uses (6). Non-active contacts are simply affected a high value.
- Longitudinal resistance of copper segments is deduced from copper resistivity (at 20T, 20K, RRR = 50) of $1.25 \times 10^{-9}\ \Omega$.m (from [8]), an approximate cross section of 10 mm^2 and longitudinal discretization dz (default dz = 1 mm).
- Superconducting resistances are classically found by $R_{sc} = E_c(I^{n-1}/Ic^n).dz$ (see [5]), and must be found iteratively

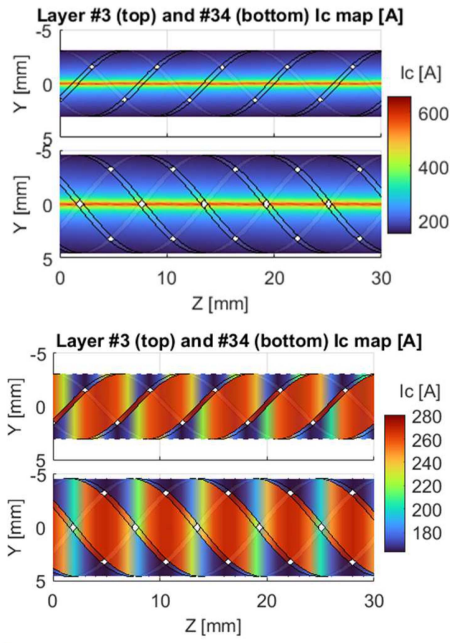

Fig. 8. Local Ic maps of Layer 3 and Layer 34 for detailed angular distribution (top) and free equipotential angular distribution for 1D network (bottom).

because of non-linearity of the E(I) relationship. I_C is known from scaling law, and for these studies the n-index is 20.

C. Superconducting Properties

As previously stated, the tapes properties were fitted on experimental data, then computed with respect to tape twisting. The resulting I_C map can be visualized on Fig. 8 .

D. Run in Operating Conditions OP1

Runs were performed on the CORC described in Fig. 3, with a modelled length of $L_{stud} = 50$ mm, and dz = 1 mm. The system matrix is 28 k × 28 k elements and CARMEN runs for about 500 s (on a personal laptop, Intel i5, 8Go RAM) to describe the full E(I) curve (∼20 currents points). The boundary conditions consider equal joint resistances in this first study. An I_C search is conducted and finds $I_C{}^{cable} = 21423$ A, which is almost exactly the HRL value. Another run with +/- 20% joint resistances took almost 10 times as much time and led to about only 3% $I_C{}^{cable}$ decrease.

After this run, here are some remarks and conclusions:

- The full redistributive model gives a cable I_C close to the HRL model. This is due to the relatively high contact resistance between tapes, but also to the very short longitudinal periodicity of the I_C in each tape which does not really permit redistribution.
- Along 50 mm, with equal joint resistances, the injected current in each tape is almost the same, with slightly more in inner layers.
- Local electric fields rise to about 6×10^{-4} V/m which is moderate, and not sufficient to redistribute by much.

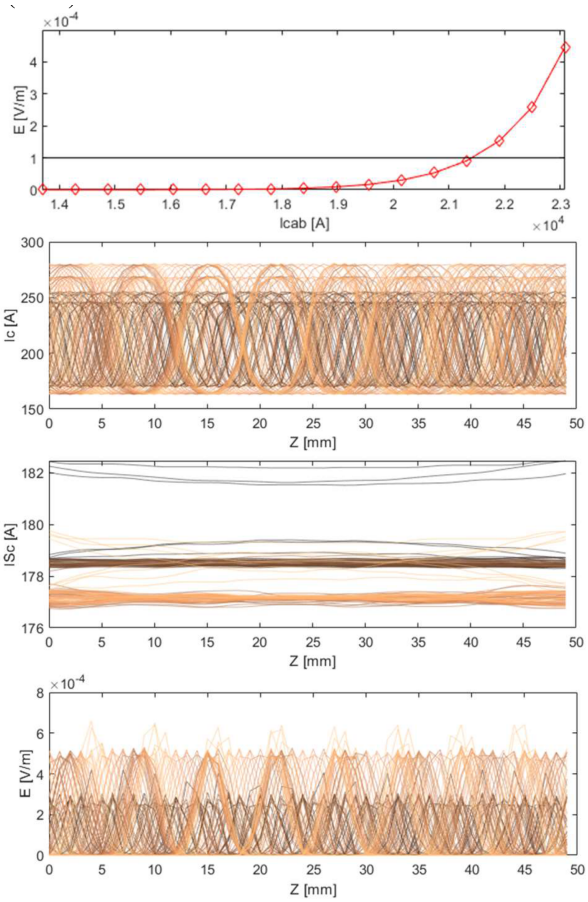

Fig. 9. Results of E(I) run on CORC cable. (a) E(I) curve, (b) longitudinal $I_C(z)$ map along each tape, (c) currents in each tape along its length, (d) Tapes local electric fields (darker are inner layers, lighters are outer layers).

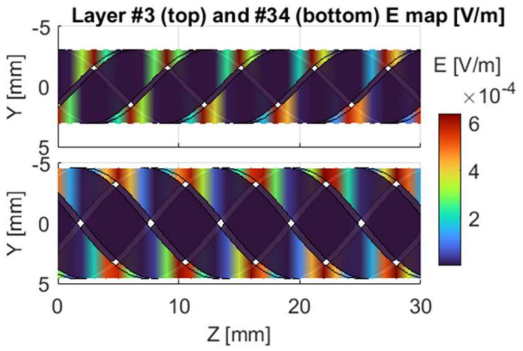

Fig. 10. Visualization of the local electric field on Layer 2 and Layer 34 (first and last superconducting layers respectively).

- Cable n-value is close to individual tapes transition index (n≈20).

A visualization of the results is also illustrating the local electric fields in Fig. 10.

VII. Conclusion

In this paper, the geometrical structure of a cylindrical REBCO cable like the CORC is studied and some important features

concerning contact lengths, areas and positions are given. Analytical electrical evaluation of the transport capacity is proposed through the LRL and HRL models. The study of a specific CORC cable using SST tapes is shown, from tapes scaling law fitting to overall cable transport capacity, including the sensitivity to local dropouts. Finally, an electrical model is developed to compute current redistributions in a 34 layers and 50 mm long sample of cable. The final computed I_C is close to the HRL limit and shows a rather low possibility to redistribute. Future work will include the sensitivity studies relating to the electrical model boundary conditions.

ACKNOWLEDGMENT

Views and opinions expressed are however those of the author(s) only and do not necessarily reflect those of the European Union or the European Commission. Neither the European Union nor the European Commission can be held responsible for them.

REFERENCES

[1] J. M. Sutcliffe, "Magnet design activities at CEA for EU-DEMO new baseline," Presented at MT29, to be published.

[2] J. Fleiter, "Development of high Tc superconducting cables for applications in CERN," Ph.D. Manuscript, 2013. [Online]. Available: https://theses.hal.science/tel-00933352v1

[3] R. Teyber et al., "Numerical investigation of current distributions around defects in high temperature superconducting CORC cables," *Supercond. Sci. Technol.*, vol. 35, 2022, Art. no. 094008.

[4] Y. Wang et al., "Quench behavior of high-temperature superconductor (RE)Ba2Cu3Ox CORC cable," *J. Phys. D: Appl. Phys.*, vol. 52, 2019, Art. no. 345303.

[5] L. Zani et al., "Code development and validation towards modeling and diagnosing current redistribution in an ITER-type superconducting cable subject to current imbalance," *Fusion Sci. Technol.*, vol. 56, pp. 690–694, 2009.

[6] D. Ciazynski and A. Torre, "Analytical formulae for computing the critical current of an Nb_3Sn strand under bending," *Supercond. Sci. Technol.*, vol. 23, 2010, Art. no. 125005.

[7] A. Torre, H. Bajas, D. Ciazynski, D. Durville, and K. Weiss, "Mechanical-electrical modeling of stretching experiment on 45 Nb_3Sn strands CICCs," *IEEE Trans. Appl. Supercond.*, vol. 21, no. 3, pp. 2042–2045, Jun. 2011.

[8] J. Fleiter and A. Ballarino, "In-field electrical resistance at 4.2 K of REBCO splices," *IEEE Trans. Appl. Supercond.*, vol. 27, no. 4, Jun. 2017, Art. no. 6603305.

[9] Cryosoft Library online documentation, "Solids," 2002. [Online]. Available: https://supermagnet.sourceforge.io/manuals/Solids_4.0.pdf

[10] V. Phifer et al., "Investigations in the tape-to-tape contact resistance and contact composition in superconducting CORC wires," *Supercond. Sci. Technol.*, vol. 35, 2022, Art. no. 065003.

[11] V. Phifer, "Experimental investigations of tape-to-tape contact resistance and its impact on current distribution around local IC degradations in CORC cables," ProQuest Dissertations & Theses, The Florida State University, 2023.